Acta Crystallographica Section F
Structural Biology and Crystallization Communications
ISSN 1744-3091

Crystallization and preliminary X-ray analysis of Pac17 from the pacidamycin-biosynthetic cluster of *Streptomyces coeruleorubidus*

Daniel R. Tromans,[a,b] Clare E. M. Stevenson,[a] Rebecca J. M. Goss[b] and David M. Lawson[a]*

[a]Department of Biological Chemistry, John Innes Centre, Norwich Research Park, Norwich NR4 7UH, England, and [b]School of Chemistry, University of East Anglia, Norwich Research Park, Norwich NR4 7TJ, England

Correspondence e-mail: david.lawson@jic.ac.uk

Received 22 May 2012
Accepted 26 June 2012

Pac17 is an uncharacterized protein from the pacidamycin gene cluster of the soil bacterium *Streptomyces coeruleorubidus*. It is implicated in the biosynthesis of the core diaminobutyric acid residue of the antibiotic, although its precise role is uncertain at present. Given that pacidamycins inhibit translocase I of *Pseudomonas aeruginosa*, a clinically unexploited antibiotic target, they offer new hope in the search for antibacterial agents directed against this important pathogen. Crystals of Pac17 were grown by vapour diffusion and X-ray data were collected at a synchrotron to a resolution of 1.9 Å from a single crystal. The crystal belonged to space group *C*2, with unit-cell parameters a = 214.12, b = 70.88, c = 142.22 Å, β = 92.96°. Preliminary analysis of these data suggests that the asymmetric unit consists of one Pac17 homotetramer, with an estimated solvent content of 49.0%.

1. Introduction

The pacidamycins (Fig. 1) are a suite of secondary metabolites produced by the Gram-positive bacterium *Streptomyces coeruleorubidus*. These compounds show an exquisitely narrow range of activity against the pathogen *Pseudomonas aeruginosa* by inhibiting the action of translocase I. Although peptidoglycan biosynthesis is a validated target for antimicrobial agents such as penicillin and vancomycin, to date compounds that specifically inhibit translocase I have not seen clinical application (Winn *et al.*, 2010). Thus, the pacidamycins offer scope for the development of new antibiotics in the fight against multidrug-resistant bacteria.

At the core of the structure of the pacidamycins is a (2*S*,3*S*)-diaminobutyric acid (DABA) moiety (Fig. 1), a nonproteinogenic amino acid that is found in a number of other natural products including the related uridyl peptide antibiotics, namely the mureidomycins (Isono & Inukai, 1991) and napsamycins (Chatterjee *et al.*, 1994), and the lipopeptide antibiotic friulimicin (Vértesy *et al.*, 2000). The pacidamycin-biosynthetic gene cluster has recently been identified in the antibiotic producer and the functions of a number of gene products have been inferred (Rackham *et al.*, 2010; Zhang *et al.*, 2010). Amongst these are Pac18 and Pac19, which are implicated in DABA biosynthesis, specifically catalysing the ATP-dependent phosphorylation of L-threonine and the conversion of the resultant phosphothreonine to DABA by a pyridoxal-phosphate-dependent β-replacement, respectively. The precise biological function of Pac17

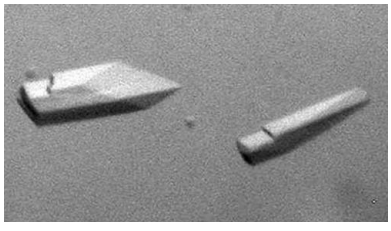

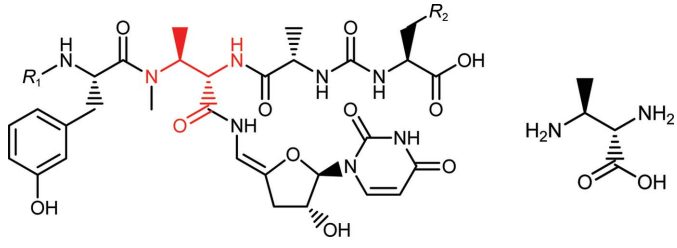

Figure 1
The pacidamycins have a common core that is decorated by groups R_1 and R_2, where R_1 is alanine, glycine or hydrogen and R_2 is indolyl, phenyl or 3-hydroxyphenyl. The central diaminobutyric acid (DABA) moiety is highlighted in red and shown separately on the right. This figure was created using *ChemDraw*.

in pacidamycin biosynthesis is uncertain. It shares significant amino-acid sequence homology to argininosuccinate lyases and the putative catalytic His and Ser residues are conserved in Pac17, whilst all of the substrate-binding residues are not (Sampaleanu *et al.*, 2002). The observation that *pac17* is translationally coupled to *pac18* and *pac19* suggests that it also plays a role in the synthesis of DABA (Rackham *et al.*, 2010; Zhang *et al.*, 2010). Homologues of Pac17 exist in the genomes of several other actinomycetes, and in at least two cases these occur in gene clusters for uridyl peptide antibiotic biosynthesis (Müller *et al.*, 2007; Kaysser *et al.*, 2011), but none of these proteins have been characterized to date.

The closest known structural homologue of Pac17, with an amino-acid sequence identity of 33% over 74% of the sequence, is argininosuccinate lyase from *Thermus thermophilus* HB8. This was used as a template to solve the Pac17 structure by molecular replacement. Here, we report the crystallization and preliminary X-ray analysis of Pac17, which represents the first of the pacidamycin-biosynthetic enzymes to be crystallized.

2. Materials and methods

2.1. Protein expression, purification and crystallization

The *pac17* gene of *S. coeruleorubidus* (UniProtKB entry E2EKP9; synonym *pacQ*) was amplified by PCR from the cosmid 2H-5 (Rackham *et al.*, 2010), which contained the minimal pacidamycin gene cluster, using a forward primer containing an *Nde*I restriction site (5′-GGACGACATATGGTGAGACTGACCGGTCGACTT-3′) and a reverse primer containing a *Bam*HI site (5′-TCCGGATCC-TCGTCAGACTCCCCCGG-3′). The amplified DNA was *Nde*I/*Bam*HI-digested and subsequently ligated into *Nde*I/*Bam*HI-digested expression vector pET28a(+) to produce the expression construct pET28a(+)Pac17, which encodes the native 498-residue Pac17 protein preceded by a thrombin-cleavable N-terminal hexahistidine tag. The inclusion of this tag appended an additional 21 amino acids onto the N-terminus of the protein with the sequence MGSS-HHHHHHSSGLVPRGSHM, giving a total molecular weight of 55 859.1 Da. The pET28a(+)Pac17 expression vector was introduced into *Escherichia coli* BL21 (DE3) cells by transformation. For protein production, 10 ml of an overnight culture of these cells was used to inoculate 1 l autoinduction medium broth containing 50 µg ml^{-1} kanamycin. The culture was grown at 310 K for 4 h and for a further 16 h at 289 K. The cells were harvested by centrifugation using a Sorvall Evolution centrifuge (15 min, 5000 rev min^{-1}, 277 K, SLC-4000 rotor) and stored at 253 K prior to purification.

All purification steps were performed at 277 K. The cell pellet was resuspended in buffer *A* (50 m*M* Tris–HCl pH 8.0, 500 m*M* NaCl, 40 m*M* imidazole) containing a Complete EDTA-free protease-inhibitor cocktail (Roche) and lysed by sonication. The supernatant and pellet were separated by centrifugation in a Sorvall Evolution centrifuge (45 min, 18 000 rev min^{-1}, 277 K, SS34 rotor). Pac17 was purified from the supernatant using a two-step procedure performed in series using an ÄKTAexpress FPLC (GE Healthcare). The sample was applied onto a 5 ml Ni^{2+}-charged His-Trap Chelating HP column (GE Healthcare), washed with 20 column volumes (CV) of buffer *A* and then eluted with 5 CV buffer *A* containing 500 m*M* imidazole at a flow rate of 4.0 ml min^{-1}. The major protein peak (based on an absorbance of >100 mAU at 280 nm) was automatically applied onto a Superdex 200 HiLoad HP gel-filtration column (GE Healthcare) in buffer *B* (20 m*M* HEPES pH 7.5, 150 m*M* NaCl) and eluted over 1.3 CV at a flow rate of 3.2 ml min^{-1}. Fractions containing the Pac17 protein (as confirmed by SDS–PAGE) were pooled and concentrated to approximately 11 mg ml^{-1} (as measured using the Bradford assay) in buffer *B* using an Amicon Ultra-15 30 kDa cutoff centrifugal concentrator (Millipore) for crystallization. The N-terminal His tag was not cleaved from the purified protein. Approximately three quarters of the protein sample was flash-frozen in liquid nitrogen as 50 µl aliquots in PCR tubes and stored at 193 K for subsequent use. The remainder was used immediately in crystallization trials.

Crystallization trials of His-tagged Pac17 were set up using an OryxNano robot (Douglas Instruments Ltd) in sitting-drop vapour-diffusion format with 96-well MRC plates (Molecular Dimensions) using a variety of commercially available screens (Hampton Research and Molecular Dimensions) at a constant temperature of 293 K. Drops consisted of 0.3 µl protein solution mixed with 0.3 µl precipitant solution and the reservoir volume was 50 µl. A number of conditions produced crystals, which were then optimized in a 24-well hanging-drop vapour-diffusion format using VDX plates (Hampton Research) with a reservoir volume of 1 ml and drops consisting of 1 µl protein solution and 1 µl precipitant solution. For each optimization, a fresh aliquot of frozen protein was used. In preparation for cryogenic data collection at the synchrotron, crystals were grown from precipitant solution supplemented with 15%(*v*/*v*) glycerol.

2.2. X-ray data collection and analysis

Crystals were mounted for X-ray data collection using LithoLoops (Molecular Dimensions), flash-cooled by plunging them into liquid nitrogen and stored in Unipuck cassettes (MiTeGen) prior to transport to the synchrotron. Crystals were subsequently transferred robotically to the goniostat on station I02 at the Diamond Light Source (Oxfordshire, England) and maintained at 100 K with a Cryojet cryocooler (Oxford Instruments). Diffraction data were recorded using an ADSC Quantum 315 CCD detector with the wavelength set to 0.9795 Å and were integrated using *XDS* (Kabsch, 2010) and scaled using *SCALA* (Evans, 2006). Further data analysis was performed using the *CCP*4 program suite (Winn *et al.*, 2011).

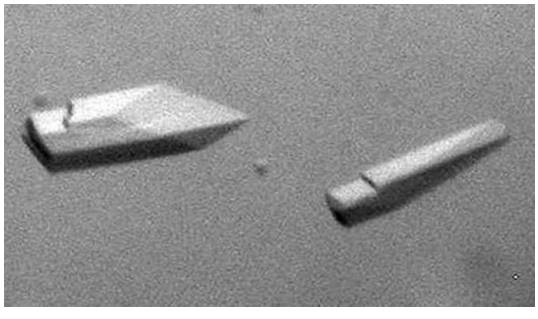

Figure 2
Crystals of Pac17 with approximate dimensions of 150 × 50 × 30 µm.

3. Results and discussion

The His-tagged Pac17 construct was overproduced and purified to greater than 95% purity as determined by SDS–PAGE analysis, with a final yield of approximately 24 mg per litre of culture. The gel-filtration column had previously been calibrated using molecular-weight gel-filtration standards (GE Healthcare). Pac17 eluted at a volume that corresponded to a molecular weight of ∼150 kDa, being indicative of a multimeric species and closest to the expected value for a homotrimer (∼168 kDa).

Crystals grew within 24 h at 293 K from a number of crystallization conditions. These conditions were optimized to improve crystal size,

with the largest crystals appearing in a precipitant solution consisting of 15%(*w*/*v*) PEG 3350, 0.2 *M* potassium sodium tartrate, 0.1 *M* bis-tris propane pH 7.5, 15%(*v*/*v*) glycerol. The largest crystals formed were approximately 150 × 50 × 30 µm in size (Fig. 2).

Native X-ray diffraction data were collected from a single Pac17 crystal: 1000 × 0.2° oscillation images were recorded in a single sweep to a maximum resolution of 1.9 Å. Indexing of the data was consistent with a *C*-centred monoclinic lattice with unit-cell parameters $a = 214.12$, $b = 70.88$, $c = 142.22$ Å, $\beta = 92.96^\circ$. The resultant reduced data set was 99.3% complete to a resolution of 1.9 Å. Data statistics are given in Table 1.

Solvent-content analysis suggested that the asymmetric unit was most likely to contain three or four His-tagged Pac17 monomers, giving estimated solvent contents of 61.8 and 49.0%, respectively (Matthews, 1968). Inspection of a self-rotation function calculated using *MOLREP* (Vagin & Teplyakov, 2010) revealed a noncrystallographic twofold axis perpendicular to *b* in the *ac* plane which, when combined with the crystallographic twofold, generates apparent 222 symmetry. This would be consistent with an asymmetric unit comprised of a 222-symmetric homotetramer. Further analysis of the data with *SFCHECK* (Vaguine *et al.*, 1999) revealed a pseudo-translation vector of 0.386, 0.000, 0.491 (fractional coordinates) at 28% of the origin peak (Fig. 3*c*).

Interrogation of the Protein Data Bank (http://www.rcsb.org/pdb) using a protein *BLAST* search revealed that the closest structural homologue was argininosuccinate lyase from *T. thermophilus* HB8 (PDB entry 2e9f; M. Goto, unpublished work), which shows 74% sequence coverage and 33% sequence identity to Pac17. The biological unit (and asymmetric unit) of the former is a homotetramer with 222 symmetry. Both monomer and tetramer polyalanine molecular-replacement templates were created from this structure using *CHAINSAW* (Stein, 2008). These were used as inputs to *Phaser* v.2.3.0 (McCoy *et al.*, 2007), which was run at 4.5 Å resolution using the default cutoffs for peak selection. With the monomer template *Phaser* reported only two solutions, each with four molecules per asymmetric unit (TFZ-equivalent scores of 36.0 and 33.4, respectively). Inspection of these solutions using *Coot* (Emsley & Cowtan, 2004) revealed them to be very similar, differing only in the placement of the subunits relative to the origin. In both cases the asymmetric unit was comprised of two equivalent 'dimers' arranged in a back-to-back fashion; after the application of crystallographic symmetry one of these dimers generated a homotetramer

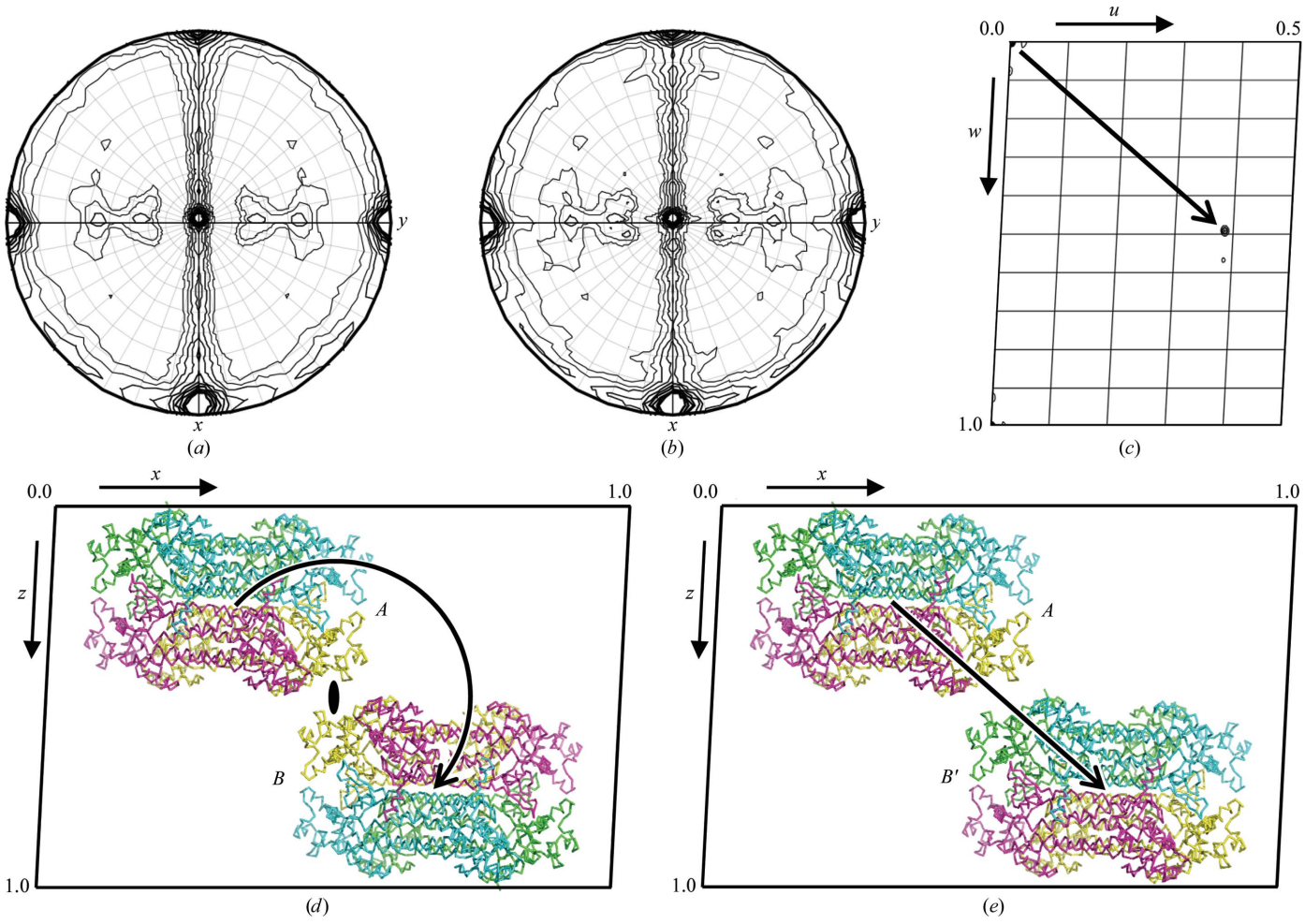

Figure 3
Preliminary crystallographic analysis of Pac17. Self-rotation functions calculated to 4.5 Å resolution from (*a*) the experimental data and (*b*) the molecular-replacement solution, showing the same noncrystallographic twofold axes ($\chi = 180^\circ$ section). Note the alignment of one of these with the crystallographic twofold axis (*y* axis). (*c*) Self-Patterson function (section $v = 0$) calculated to 4.5 Å resolution from the experimental data, revealing a clear pseudotranslation vector of 0.386, 0.000, 0.491 (fractional coordinates). The alignment of crystallographic and noncrystallographic twofold axes gives rise to similarly oriented tetramers in the unit cell. Specifically, (*d*) the application of twofold crystallographic symmetry (operator: $1 - x, y, 1 - z$) generates tetramer *B* from tetramer *A*, which is essentially equivalent to (*e*) the translation of molecule *A* by the pseudotranslation vector to give molecule *B*′. For clarity, only two of the four copies of the tetramer in the unit cell are shown in (*d*) and (*e*). (*d*) and (*e*) were created using *PyMOL* (DeLano, 2002).

Table 1
Summary of X-ray data for Pac17.

Values in parentheses are for the outer resolution shell.

No. of crystals	1
Beamline	I02, Diamond Light Source
Wavelength (Å)	0.9795
Detector	ADSC Quantum 315 CCD
Crystal-to-detector distance (mm)	290.7
Rotation range per image (°)	0.2
Exposure time per image (s)	0.25
Beam transmission (%)	27.2
Total rotation range (°)	200.0
Resolution range (Å)	67.28–1.90 (2.00–1.90)
Space group	*C*2
Unit-cell parameters (Å, °)	a = 214.12, b = 70.88, c = 142.22, β = 92.96
Estimated mosaicity (°)	0.2
Total No. of measured intensities	672568 (74768)
Unique reflections	166584 (23088)
Multiplicity	4.0 (3.2)
Mean $I/\sigma(I)$	8.5 (2.0)
Completeness (%)	99.3 (95.1)
$R_{\rm merge}$†	0.127 (0.583)
$R_{\rm meas}$‡	0.147 (0.704)
$CC_{1/2}$§	0.994 (0.706)
Wilson B value (Å^2)	15.6

† $R_{\rm merge} = \sum_{hkl}\sum_i |I_i(hkl) - \langle I(hkl)\rangle| / \sum_{hkl}\sum_i I_i(hkl)$. ‡ $R_{\rm meas} = \sum_{hkl}\{N(hkl)/[N(hkl)-1]\}^{1/2}\sum_i |I_i(hkl) - \langle I(hkl)\rangle| / \sum_{hkl}\sum_i I_i(hkl)$, where $I_i(hkl)$ is the ith observation of reflection hkl, $\langle I(hkl)\rangle$ is the weighted average intensity for all observations i of reflection hkl and N is the number of observations of reflection hkl. § $CC_{1/2}$ is the correlation coefficient between intensities from random halves of the data set.

corresponding to the biological unit of the template structure, whilst the other dimer did not generate a homotetramer and in fact partially overlapped with crystallographically related dimers (PAK scores of 73 and 68 for the two solutions, respectively). With the tetramer template, only a single solution was reported (TFZ-equivalent score of 49.4). This was judged to be a correct solution because (i) the packing looked reasonable, *i.e.* there were no clashes (PAK score = 0) and no large gaps in the lattice, (ii) a self-rotation function calculated from the model structure factors (Fig. 3*b*) was consistent with that calculated from the experimental structure factors (Fig. 3*a*), indicating that the twofold axes of the model were correctly oriented, and (iii) since one of the model twofold axes was parallel to the crystallographic twofold axis (Fig. 3*a*), the application of twofold crystallographic symmetry resulted in similarly oriented tetramers within the same unit cell (Fig. 3*d*), which were therefore also related by translational symmetry alone (Fig. 3*e*). The corresponding translational vector agreed with that reported by *SFCHECK* (Fig. 3*c*). Rigid-body refinement of this model at 4.5 Å resolution using *REFMAC*5 (Murshudov *et al.*, 2011) gave an $R_{\rm free}$ value of 0.547, a free correlation coefficient of 0.525 and a figure of merit of 0.393.

Subsequent analysis of the *Phaser* solutions generated from the monomer template indicated that in both cases all four subunits were correctly oriented and the two dimers corresponded to halves of the biological unit. It is not clear why *Phaser* failed to correctly combine the two dimers in the translation function, but it may have been influenced by the pseudo-symmetry, or perhaps in some way 'confused' by the densely packed core of the homotetramer, which is comprised of 20 long roughly parallel α-helices (five per subunit). Indeed, this densely packed core, and the distinctly nonspherical overall shape of the assembly, could account for the anomalously low estimate of the multimeric state from the gel-filtration column.

Rebuilding and refinement of the preliminary Pac17 model are under way. A full description of this process and analysis of the resultant structure will be reported elsewhere. This work represents the first step towards a full structural and functional characterization of Pac17.

We thank the Norwich Research Park for a studentship (awarded to DRT) and the Biotechnology and Biological Sciences Research Council for support through grants BB/I022910/1 (to RJMG) and BB/J004561/1 (to the John Innes Centre) and from the John Innes Foundation. We are grateful for the support of the Diamond Light Source and for the assistance of the beamline scientists at station I02. S. Grüschow is acknowledged for helpful advice and technical assistance.

References

Chatterjee, S., Nadkarni, S. R., Vijayakumar, E. K., Patel, M. V., Ganguli, B. N., Fehlhaber, H. W. & Vertesy, L. (1994). *J. Antibiot.* **47**, 595–598.
DeLano, W. L. (2002). *PyMOL*. http://www.pymol.org.
Emsley, P. & Cowtan, K. (2004). *Acta Cryst.* D**60**, 2126–2132.
Evans, P. (2006). *Acta Cryst.* D**62**, 72–82.
Isono, F. & Inukai, M. (1991). *Antimicrob. Agents Chemother.* **35**, 234–236.
Kabsch, W. (2010). *Acta Cryst.* D**66**, 125–132.
Kaysser, L., Tang, X., Wemakor, E., Sedding, K., Hennig, S., Siebenberg, S. & Gust, B. (2011). *Chembiochem*, **12**, 477–487.
Matthews, B. W. (1968). *J. Mol. Biol.* **33**, 491–497.
McCoy, A. J., Grosse-Kunstleve, R. W., Adams, P. D., Winn, M. D., Storoni, L. C. & Read, R. J. (2007). *J. Appl. Cryst.* **40**, 658–674.
Müller, C., Nolden, S., Gebhardt, P., Heinzelmann, E., Lange, C., Puk, O., Welzel, K., Wohlleben, W. & Schwartz, D. (2007). *Antimicrob. Agents Chemother.* **51**, 1028–1037.
Murshudov, G. N., Skubák, P., Lebedev, A. A., Pannu, N. S., Steiner, R. A., Nicholls, R. A., Winn, M. D., Long, F. & Vagin, A. A. (2011). *Acta Cryst.* D**67**, 355–367.
Rackham, E. J., Grüschow, S., Ragab, A. E., Dickens, S. & Goss, R. J. M. (2010). *Chembiochem*, **11**, 1700–1709.
Sampaleanu, L. M., Yu, B. & Howell, P. L. (2002). *J. Biol. Chem.* **277**, 4166–4175.
Stein, N. (2008). *J. Appl. Cryst.* **41**, 641–643.
Vagin, A. & Teplyakov, A. (2010). *Acta Cryst.* D**66**, 22–25.
Vaguine, A. A., Richelle, J. & Wodak, S. J. (1999). *Acta Cryst.* D**55**, 191–205.
Vértesy, L., Ehlers, E., Kogler, H., Kurz, M., Meiwes, J., Seibert, G., Vogel, M. & Hammann, P. (2000). *J. Antibiot.* **53**, 816–827.
Winn, M., Goss, R. J. M., Kimura, K. & Bugg, T. D. (2010). *Nat. Prod. Rep.* **27**, 279–304.
Winn, M. D. *et al.* (2011). *Acta Cryst.* D**67**, 235–242.
Zhang, W., Ostash, B. & Walsh, C. T. (2010). *Proc. Natl Acad. Sci. USA*, **107**, 16828–16833.